Hindawi
Journal of Advanced Transportation
Volume 2017, Article ID 3192967, 8 pages
https://doi.org/10.1155/2017/3192967

*Research Article*

# Turnout Fault Diagnosis through Dynamic Time Warping and Signal Normalization

**Shize Huang,[1] Fan Zhang,[1] Rongjie Yu,[1,2] Wei Chen,[1] Fei Hu,[3] and Decun Dong[1]**

[1] *Key Laboratory of Road and Traffic Engineering of Ministry of Education, Tongji University, Shanghai 201804, China*
[2] *State Key Laboratory of Rail Traffic Control and Safety, Beijing Jiaotong University, Beijing 100044, China*
[3] *Department of Electrical and Computer Engineering, University of Alabama, Tuscaloosa, AL 35487, USA*

Correspondence should be addressed to Rongjie Yu; yurongjie@tongji.edu.cn

Received 30 May 2017; Revised 27 August 2017; Accepted 20 September 2017; Published 23 October 2017

Academic Editor: N. N. Sze



Turnout is one key fundamental infrastructure in the railway signal system, which has great influence on the safety of railway systems. Currently, turnout fault diagnoses are conducted manually in China; engineers are obliged to observe the signals and make problem solving decisions. Thus, the accuracies of fault diagnoses totally depend on the engineers' experience although massive data are produced in real time by the turnout microcomputer-based monitoring systems. This paper aims to develop an intelligent diagnosis method for railway turnout through Dynamic Time Warping (DTW). We firstly extract the features of normal turnout operation current curve and normalize the collected turnout current curves. Then, five typical fault reference curves are ascertained through the microcomputer-based monitoring system, and DTW is used to identify the turnout current curve fault through test data. The analysis results based on the similarity data indicate that the analyzed five turnout fault types can be diagnosed automatically with 100% accuracy. Finally, the benefits of the proposed method and future research directions were discussed.

## 1. Introduction

Recently, the railway system has experienced rapid development all over the world [1] with both the freight and passenger traffic demands increasing. According to a report from the National Railway Administration of the People's Republic of China, the railway passenger and cargo transportation volume in China were 2.535 billion and 3.358 billion tons, respectively, in 2015 [2]. Therefore, due to the rapid development, the maintenance of the railway system has become a critical issue. Problems such as lack of relevant experienced professionals and heavy workloads to monitor the railway safety are emerging.

Turnout (shown in Figure 1), with high operation frequency, is the core component of the railway infrastructure since it is an essential device which moves the train from one track to another [3]. Turnout failures have caused several major railway accidents recently [4]. According to one report, more than 100 turnout failure events occurred in Changsha communication and signal division each year, and this accounted for 17.5% of all faults of the signaling equipment including turnout in the past five years [5].

Given the importance of the turnout system, microcomputer-based monitoring system (MMS) has been introduced to monitor the turnout state in real time in China. The MMS collects turnout operation current and voltage levels data; then engineers perform the failure diagnose analysis based on the displayed curves. The current manual diagnosis system has not only caused low diagnosis efficiency, but also increased the manpower and resources requirements [6]. In addition, the accuracy of the diagnosis mainly depends on the engineers' subjective experiences, where any misinterpretation of the data could lead to potential safety issues. Therefore, automatic turnout pattern detection methods are needed to identify the railway faults or failures.

Given the emerging issue, different methods have been utilized in the turnout failure diagnosis area. Zhao and Lu

Figure 1: Turnout system.

studied the turnout fault diagnosis system based on gray correlation analysis [7]. Roberts et al. used single throw mechanical equipment (STME) to detect the fault [8]. Neural network and fuzzy theory ([9–13]), Support Vector Machine (SVM), and improved SVM ([6, 14]) have also been applied for turnout fault diagnoses. Atamuradov et al. utilized Dynamic Time Warping (DTW) and expert systems to recognize three states including one healthy state and two failure states for turnout [15]. Ardakani et al. established the health assessment of the turnout by Principal Component Analysis (PCA) [16].

However, the abovementioned methods have several limitations for the targeted problem. For example, gray correlation analysis needs to choose suitable feature vectors or parameters that are hard to ascertain for large scale of fault types since a continuous search of large space is needed until the matching feature vector or parameter is identified. Besides, SVM-based methods cannot efficiently handle the large sample size. And expert system needs to have much a priori knowledge, which requires much manpower from experienced people to summarize the rules and knowledge based on years of experience. However, it is difficult to build a complete knowledge base due to more microcomputer-based monitoring systems and various environments and lack of rich experience. Besides, neural network and fuzzy theory models were developed based on large size of historical fault data, which is difficult to collect, and the model training process would be time consuming for tuning the model parameters.

Recently, Dynamic Time Warping (DTW) [17], a Dynamic Programming (DP) method which has originally been used in isolated word recognition area, has become popular. DTW calculates the distance between reference data and test data which has never been trained, and the smallest distance indicates the greatest similarity [18–20]. And it holds the benefits of requiring small amount of fault reference data, no need of selecting feature vectors, and requiring limited historical data and a priori knowledge. In this study, DTW was introduced to conduct the turnout fault diagnosis.

In addition to the analysis method, various data have been used in the literature, such as turnout operation current [21–23], turnout operation power [24], and data from sensors [25–27]. Most researchers choose the first two kinds of data since they can be obtained directly by the MMS. Moreover, the data from sensors requires the installation of extra sensors, which may be cost-prohibitive. Therefore, in this study, we utilize turnout operation current data to analyze the fault because current data can intuitively reflect the turnout fault while power data cannot.

Conventional methods to diagnose the fault based on turnout operation current data do not deal with current curve images. The turnout comes from different manufacturers, disparate MMSs, and diverse railway bureaus. Thus, the current curves images have much disturbance such as noise and grids which may seriously affect the accuracy of diagnosis results. Through the normalization of the current curve [28], we can effectively remove the noise in the image and diagnose the types of turnout faults.

Furthermore, in this study the single-action ZD6 turnout will be targeted given its wide range of applications. The operation current curves were collected from the MMS. We will first normalize the original turnout operation current curve and ascertain turnout reference templates. Then, the similarities between the reference templates and the test samples will be calculated through DTW. Each turnout diagnosis result would be recorded and finally the classification accuracy of the proposed approach will be evaluated.

The rest of this paper is organized as follows. Section 2 provides the meaning of the normal turnout operation current curve for each stage and introduces the method of image normalization method for turnout current curves. The method and principles of DTW and reference templates are explained in Section 3. Section 4 presents numerical experiments and result for the real turnout operation current curves to diagnose the faults, followed by the conclusions and discussions in Section 5.

## 2. Data Preparation

*2.1. Turnout Operation Current Curve.* Nowadays, MMS is the main approach to monitor the state of the turnout in China. Turnout operation current curve can intuitively reflect current changes of the switch machine. The operation process of the turnout can be divided into four stages: unlocking, conversion, locking, and slow release [12]. We can see the characteristics of the turnout operation current curve of different stages from Figure 2:

(1) Stage 1 (unlocking) ($T_0$-$T_1$): the motor starts with a large starting current which makes the curve rise suddenly. With the operation of the turnout system, the curve shows sharp decline and the turnout enters the unlocking stage.

(2) Stage 2 (conversion) ($T_1$-$T_2$): the current curve is smooth because the turnout operates smoothly during the conversion process.

(3) Stage 3 (locking) ($T_2$-$T_3$): the point moves to the other side of the rail and the current curve reduces to zero when the locking stage is finished.

(4) Stage 4 (slow release) ($T_3$-$T_4$): 1DQJ relay slows release and the current stays at zero continuously at slow release stage.

*2.2. Image Standardization.* Turnout operation current curves collected from different MMSs, diverse railway bureaus and various environments, may have much disturbance which causes fault detection errors. It is indispensable to process

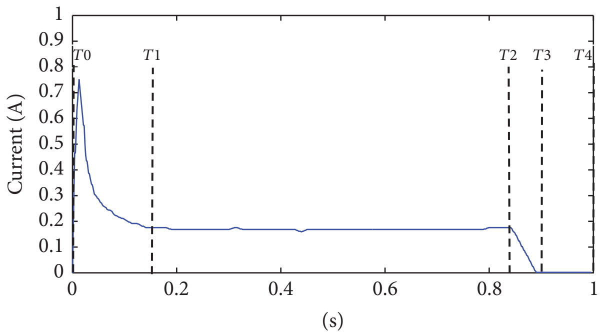


Figure 2: The turnout operation current curve.

turnout operation current curves and improve the accuracy of fault diagnosis. We need to remove the noise such that the disturbance in the images does not affect the experimental results. We have used the following procedure to remove the noise:

(1) Gray-scale transformation: it is a method of producing the gray value for each pixel of the original image according to a target condition. The gray value of the original image pixel is assumed as

$$D = f(x, y), \tag{1}$$

where $D$ is the gray value of the original image pixel andxis abscissa andyis ordinate. Gray-scale enhancement is expressed as

$$f(x, y) = T[g(x, y)] \tag{2}$$

and $g(x, y)$ is the function of the image threshold.

(2) Binarization: the gray-scale image is converted into binary image which is a two-dimensional array ($M \times N$). The value of the pixel is set to 0 if the gray value is less than the threshold $T$; otherwise the value of the pixel is set to 1. The function of the image threshold is

$$g(x, y) = \begin{cases} 0 & f(x, y) \le T \\ 1 & f(x, y) > T. \end{cases} \tag{3}$$

(3) Noise removal: the first step is to find out the target region surrounded by the axis through the sum of the rows and columns in the two-dimensional array. Then isolated pixels are removed from the object region with open operations including erosion and dilation.

(4) Refinement: the denoising image may have multiple zero pixels in one column. And this situation would lead to the phenomenon that a moment corresponds to a number of current values in the coordinate transformation. It is assumed that the value of $L$ pixel is 0, and the value $R$ in that row is

$$R = \{r_1, r_2, r_3, \ldots, r_L\} \tag{4}$$

and $r_1$ is the value of 1 pixel.

The number of rows in the $k$th column with the value of pixel of 0 is

$$r_K = \frac{\sum_{i=1}^{L} r_i}{L} \tag{5}$$

and others are set to 1.

(5) Coordinate transformation: the purpose of the coordinate transformation is to convert the coordinate of the curve from the RO'C coordinate system to the tO'I coordinate system. We assume that the point $M$ with coordinate $(c_m, r_m)$ in the RO'C coordinate system has $(t_m, I_m)$ in the tO'I coordinate system. Thus

$$\begin{gathered} \left(\frac{OM_1}{OB}\right)_{\text{RO'C}} = \left(\frac{OM_1}{OB}\right)_{\text{tO'I}} \\ \left(\frac{OM_2}{OA}\right)_{\text{RO'C}} = \left(\frac{OM_2}{OA}\right)_{\text{tO'I}}. \end{gathered} \tag{6}$$

Point coordinate is

$$\begin{gathered} \left(\frac{c_m - c_1}{c_2 - c_1}\right) = \left(\frac{t_m - t_0}{t_b - t_0}\right) \\ \left(\frac{r_2 - r_m}{r_2 - r_1}\right) = \left(\frac{I_m - I_0}{I_a - t_0}\right). \end{gathered} \tag{7}$$

$c_1$, $c_2$, $r_1$, and $r_2$ are the edge line of location for the target area and $t_0$, $I_0$, $t_a$, $I_a$, $t_b$, and $I_b$ are set by engineers.

(6) Normalization: the normalization aims to zoom the data proportionally and place it in a specific interval in order to make the algorithm universal because the data comes from disparate systems and manufacturers. It eliminates the influence of different coordinates. For example, the range of t in one image is 0 to 5 and in another it is 0 to 8. The same type of switch machine made in different factories has different current values but the turnout operation current curves have the same tendency. The original data is transformed linearly and the results are mapped to $[0, 1]$. The transformation function is as follows:

$$X' = \frac{X - X_{\min}}{X_{\max} - X_{\min}}. \tag{8}$$

And $X'$ is a point after normalization. $X$ is original data. $X_{\max}$ is the maximum value. $X_{\min}$ is the minimum value.

The normalization process is shown in Figure 3. All of reference templates and test samples must be processed.

## 3. Methodology

*3.1. Dynamic Time Warping (DTW).* In this study, DTW was used to calculate the similarities between test samples and reference templates in order to diagnose the fault types.

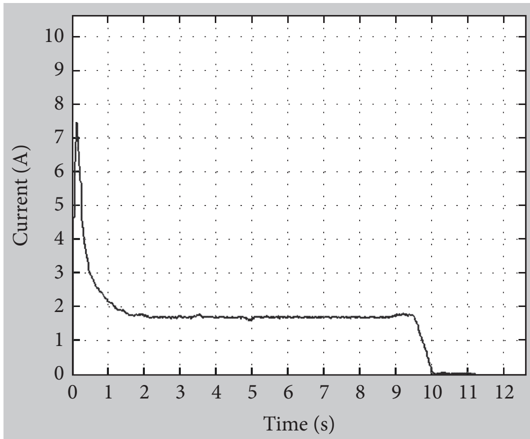


(a) Gray-scale transformation

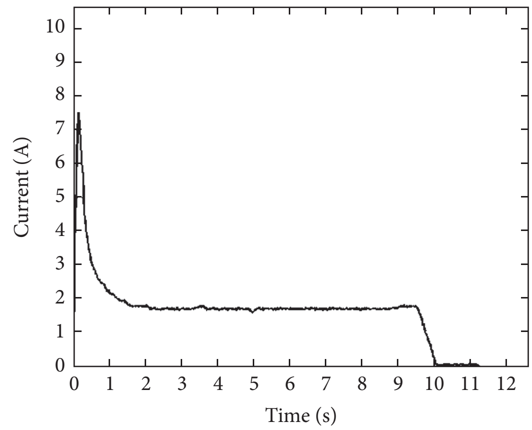


(b) Binarization

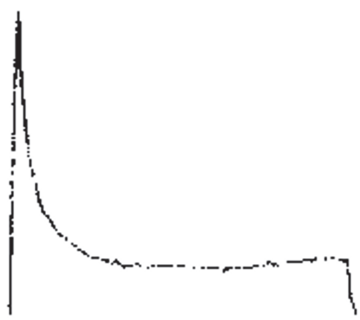

(c) Noise removal

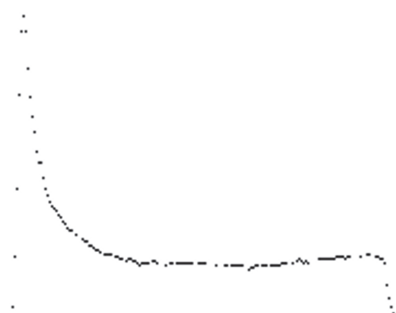

(d) Refinement

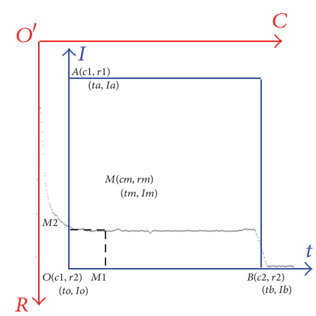


(e) Coordinates transformation

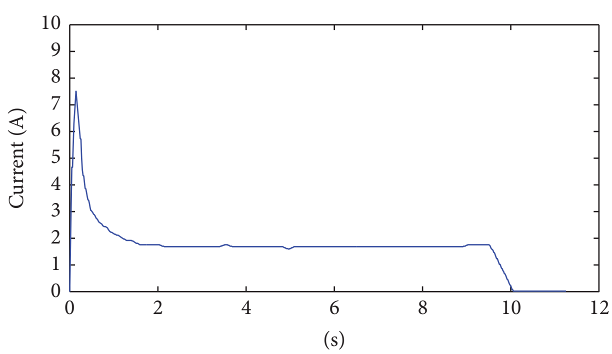


(f) Normalization

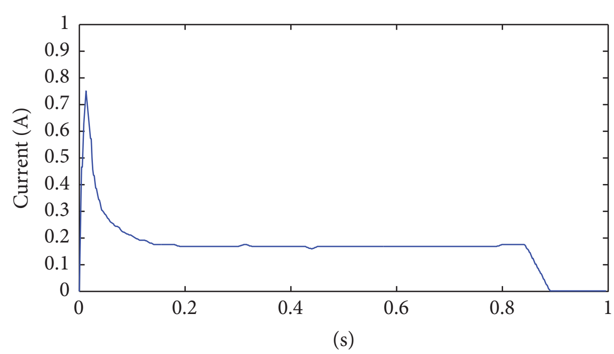


(g) Normalized image

Figure 3: Image normalization process.

DTW was firstly introduced in the field of speech recognition to recognize the distortion of similar sounds, and it was a flexible distance-based curve comparison model which has been successfully applied to a wide range of time series data [17]. DTW is based on the idea of Dynamic Programming (DP), which can match different lengths of the time series and avoid mismatch between the peaks on curves even if the abscissa of peak is different. In Figure 4, the peak of the top line is point $a$. It is incorrect to simply consider that point $a$ would correspond to point $b'$ in the bottom curve. DTW can identify point $b$ which corresponds to point $a$ and then calculate the distance of two lines. It compares the similarity of two series by calculating a similarity matrix and searching for an optimal path with the minimum cumulative distance.

The path is not casually selected. The selected path must start from the lower left corner and end in the upper right corner, as shown in Figure 5. It is assumed that the grid points in the path are $(n_1, m_1), \ldots, (n_i, m_j), \ldots, (n_N, m_M)$. If the path has passed the point $(n, m)$, the next passing point can only be one of the following three cases:

(1) $(n, m) = (n + 1, m)$.

(2) $(n, m) = (n + 1, m + 1)$.

(3) $(n, m) = (n, m + 1)$.

The path starts from the point (0, 0) to match the two sequences $T$ and $R$. All the distances of points calculated before will be accumulated when it is reaching each point.

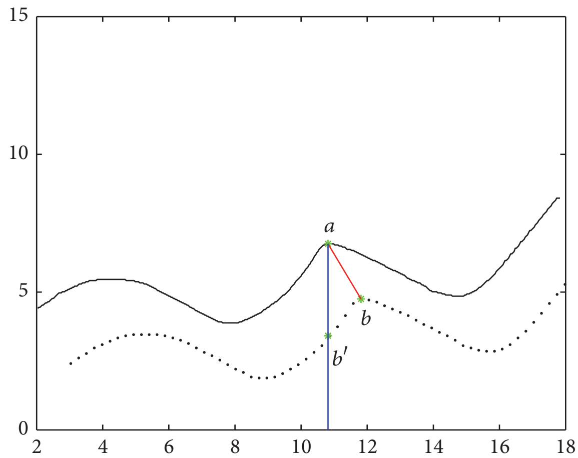


Figure 4: Match the peaks by using DTW.

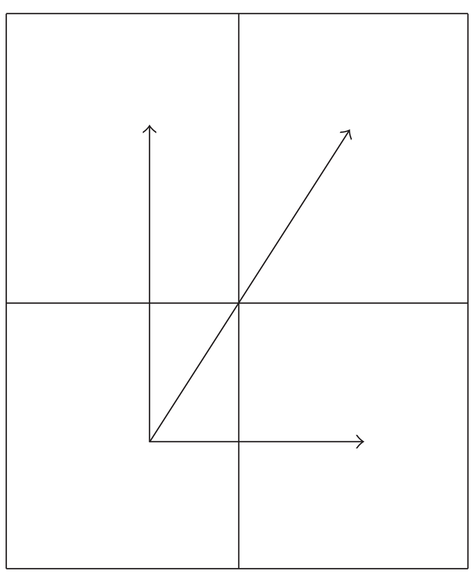

Figure 5: The selected path.

After reaching the end point $(n, m)$, the optimal path is formed and the cumulative distance is the last total distance. The lower the cumulative distance between the time sequences is, the higher the similarity is [14]. Thus the minimum cumulative distance of the time sequences $T$ and $R$ is

$$D[(n,m)] = d[T(n), R(m)] + \min\{D(n+1,m), D(n+1,m+1), D(n,m+1)\}. \tag{9}$$

DTW algorithm compares the test samples with the reference templates directly without the need of knowing plenty of prior knowledge and historical data. It is a kind of practical method for fault diagnosis because this algorithm only needs several reference templates to diagnose the fault.

*3.2. Confirming Reference Templates.* A total of 5 ZD6 turnout fault type current curves were selected as the reference templates, which are shown in Figure 6.

Figure 6(a) presents the fault that the turnout suddenly stops running after starting. It can be seen that conversion time is short and locking line disappears. There are several potential reasons for that: (1) The switch machine action current is too small. (2) The switch machine has a poor performance. (3) The self-closing circuit of 1DQJ has faults that 1DQJ cannot continue after sucking up. The end of turnout jamming curve in Figure 6(b) is stable at a relatively high value. The reason for this is that there is foreign matter between the switch rail and the stock rail or the fault current of the switch machine is too small. Figure 6(c) shows the current curve when start-up circuit disconnects. The trend of this curve is almost straight without parabolic downward trend and the value of current stays at a high value. This failure is due to the mixed line of stator and rotor. Exceeding locking current curve (shown in Figure 6(d)) suddenly rises in the locking section. The reasons for this could be tight turnout adjustment, dirty slide plate, lack of oil in slide plate, the stock rail with a lateral move, and so on. Figure 6(e) shows the fault that automatic actuator is not flexible. This locking line of fault current curve is longer than normal curve and has a larger current value. The reason is that the turnout has been already locked and several shafts of the automatic actuator action are not flexible due to lack of oil. It causes the following: the automatic actuator operation becomes abnormal and the start connections cannot be disconnected.

## 4. Performance Analysis

In this study, a total of 260 current curves have been tested to verify the accuracy of proposed analysis method. Each test sample was compared with the 6 preselected reference templates including one normal template and 5 fault templates through DTW algorithm. Smaller distances between the test sample and reference templates indicate larger similarity. Shown as an example, the distances for 10 current curves between test samples and 6 kinds of reference templates are shown in Table 1. The system fault identification results are shown in Table 2.

From Table 1, we can find the smallest values in each row. That means that this curve has great similarity to the reference template where the smallest numbers are located. Thus, curves (1) and (9) indicate turnout jamming. Curves (2) and (6) represent that the turnout suddenly stops running after starting. Start-up circuit disconnection corresponds to curves (3) and (10). Exceeding locking current is for curves (5) and (8). Curves (4) and (7) indicate that automatic actuator is not flexible. We have verified in real experiments that all of our fault identification results are correct.

Table 2 shows the diagnosis results for the system. Each type of faults has 52 curves and the normal curve is 0 for total of 260 test samples.

Table 3 presents the accuracy of the system diagnosis result for 5 kinds of faults, and a 100% accuracy rate was achieved, while, in [15], the classification accuracy of fault detection decreased along with the increase of noise level. In this study, image normalization procedure is used to avoid the impact of noise and other interference on the result, and

Table 1: The distance between test samples and reference templates.

| Curve | Normal | Turnout suddenly stops running after starting | Turnout jamming | Start-up circuit disconnection | Exceeding locking current | Automatic actuator is not flexible |
|---|---|---|---|---|---|---|
| (1) | 83.74164 | 85.27251 | 0.07067 | 893.41762 | 138.01478 | 103.46032 |
| (2) | 73.65857 | 4.16262 | 1.79*e* + 308 | 1.79*e* + 308 | 1.79*e* + 308 | 1.79*e* + 308 |
| (3) | 137.36763 | 35.84982 | 482.30596 | 0.67117 | 271.46292 | 1.79*e* + 308 |
| (4) | 139.69423 | 110.73194 | 108.16510 | 1179.04733 | 68.79076 | 0.92959 |
| (5) | 157.70522 | 205.33733 | 316.96448 | 978.42134 | 85.86655 | 198.50005 |
| (6) | 79.33443 | 5.60595 | 1.79*e* + 308 | 1.79*e* + 308 | 1.79*e* + 308 | 1.79*e* + 308 |
| (7) | 124.28016 | 95.15331 | 107.97440 | 1199.03284 | 62.16355 | 2.54591 |
| (8) | 169.02205 | 216.35205 | 324.22023 | 1001.80220 | 97.32649 | 204.93660 |
| (9) | 79.1762 | 81.5792 | 0.3843 | 888.6765 | 134.7714 | 105.8146 |
| (10) | 132.39715 | 33.21258 | 464.77556 | 1.59861 | 261.00913 | 1.797*e* + 308 |

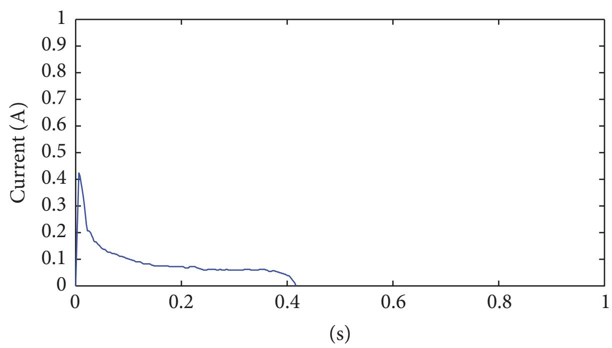


(a) Turnout suddenly stops running after starting

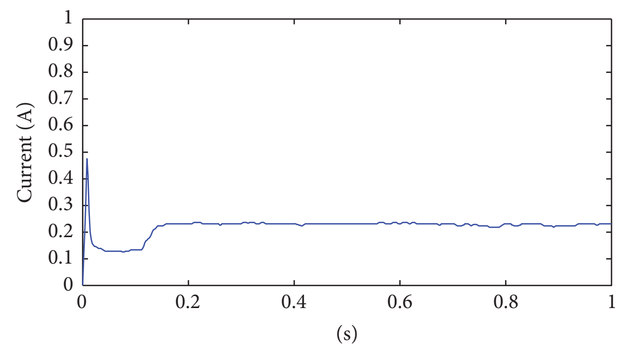


(b) Turnout jamming

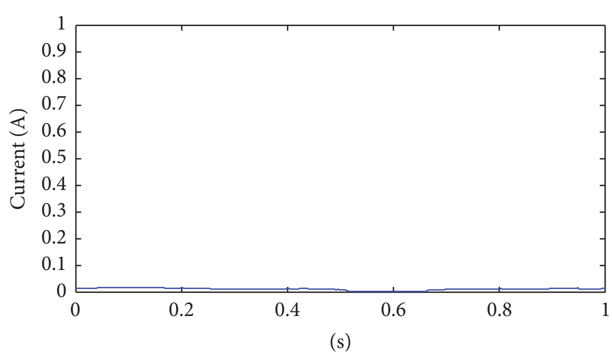


(c) Start-up circuit disconnection

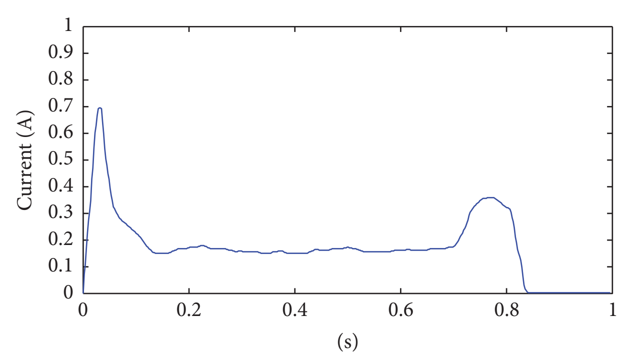


(d) Exceeding locking current

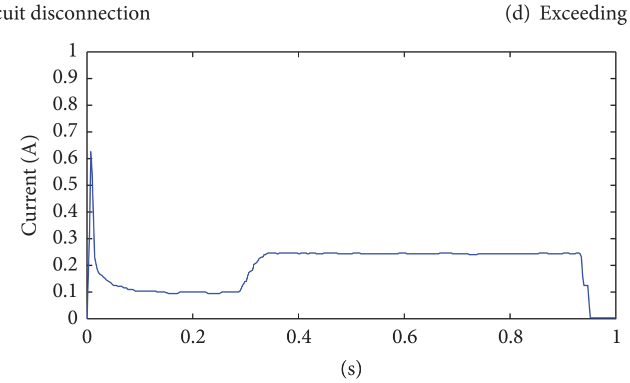


(e) Automatic actuator is not flexible

Figure 6: Turnout fault current curves.

Table 2: The number of different kinds of curves.

| Type of curves | Normal | Turnout suddenly stops running after starting | Turnout jamming | Start-up circuit disconnection | Exceeding locking current | Automatic actuator is not flexible |
|---|---|---|---|---|---|---|
| Number of curves | 0 | 52 | 52 | 52 | 52 | 52 |

Table 3: Accuracy of fault diagnosis.

| Type | Turnout suddenly stops running after starting | Turnout jamming | Start-up circuit disconnection | Exceeding locking current | Automatic actuator is not flexible |
|---|---|---|---|---|---|
| Accuracy | 100% | 100% | 100% | 100% | 100% |

DTW scheme can greatly improve the diagnosis efficiency and accuracy without using other algorithms, rules, or a priori knowledge.

## 5. Discussion and Conclusions

In this study, we have developed an automatic fault diagnostic method based on DTW scheme for the railway turnouts. Firstly, all the turnout current curves captured from the MMS were normalized, and both normal and fault reference templates were identified. Then, a total of 260 turnout current curves which have never been trained were compared with 6 reference templates through DTW scheme. By seeking the minimum cumulative distance between test samples and reference templates, various fault types were identified. The analysis results indicated that the turnout faults could be diagnosed through the proposed method automatically with 100% accuracy for 5 typical fault current curves. Our scheme could avoid accidents caused by new-joined or less experienced technicians' errors and saves much manpower and material resources to improve the railway safety.

In a previous study [15], DTW was also used to analyze a similar problem; however, the analysis results showed that noises in the curves have significantly impacted the accuracy of the result, and the accuracy of system decreases as the noise level increases. This further reduces the system reliability and could even cause accidents because of fault misclassification. Unlike the previous study, in this study, a curve normalization procedure was used to eliminate the impacts of noises. In addition, Atamuradov et al. [15] used some rules to diagnose the turnout failure. However, rule-based system lacks flexibility, since the data from different MMSs may have built-in heterogeneity. In this study, the results indicate that the developed method can diagnose multiple kinds of turnout faults even if the values of current curve fluctuate much and the operation time of turnout is different. Besides, DTW does not require feature vector selection, historical data, or a priori knowledge, which is beneficial for real-time diagnosis.

Our next work would be investigating other algorithms (such as cluster algorithm or manifold learning or deep learning) to recognize the undefined type of turnout fault. Besides, big data learning issues will also be investigated since the collected current or voltage curves are extremely large in data size.

## Conflicts of Interest

The authors declare that they have no conflicts of interest.

## Acknowledgments

This research is supported by National Key R&D Program of China (2016YFB1200402), National Natural Science Foundation of China (61703308 and 71401127), and the State Key Laboratory of Rail Traffic Control and Safety (Contract no. RCS2017K003), Beijing Jiaotong University.

## References

[1] X. Yang, X. Li, B. Ning, and T. Tang, "A survey on energy-efficient train operation for urban rail transit," *IEEE Transactions on Intelligent Transportation Systems*, vol. 17, no. 1, pp. 2–13, 2016.

[2] *Rail-way statistical bulletin in 2015*, National Railway Administration of the People's Repubilc of China, 2016, http://www.nra.gov.cn/fwyd/zlzx/hytj/.

[3] A. Morant, P.-O. Larsson-Kråik, and U. Kumar, "Data-driven model for maintenance decision support: A case study of railway signalling systems," *Proceedings of the Institution of Mechanical Engineers, Part F: Journal of Rail and Rapid Transit*, vol. 230, no. 1, pp. 220–234, 2016.

[4] *Selection of railway traffic accident case*, China Railway Press, Ministry of Railways of the People's Republic of China, Beijing, China, 1999, 27–87.

[5] G. Wang, T. Xu, T. Tang, T. Yuan, and H. Wang, "A Bayesian network model for prediction of weather-related failures in railway turnout systems," *Expert Systems with Applications*, vol. 69, pp. 247–256, 2017.

[6] F. Zhou, L. Xia, W. Dong, X. Sun, X. Yan, and Q. Zhao, "Fault diagnosis of high-speed railway turnout based on support vector machine," in *Proceedings of the International Conference on Industrial Technology (ICIT*, pp. 1539–1544, May 2016.

[7] L.-H. Zhao and Q. Lu, "Method of turnout fault diagnosis based on grey correlation analysis," *Journal of the China Railway Society*, vol. 36, no. 2, pp. 69–74, 2014.

[8] C. Roberts, H. P. B. Dassanayake, N. Lehrasab, and C. J. Goodman, "Distributed quantitative and qualitative fault diagnosis: Railway junction case study," *Control Engineering Practice*, vol. 10, no. 4, pp. 419–429, 2002.

[9] Y. Q. Zhai, *Research on Bayesian Networks in the Application of Rail Switch Control Circuit Fault Diagnosis*, Lanzhou Jiaotong University, 2012, 1–59.

[10] T. J. Wang and D. Yu, "Based on BP neural network turnout intelligent fault diagnosis method," *Journal of Railway Operation Technology*, vol. 17, no. 2, pp. 4–7, 2011.

[11] Y. M. Li and W. J. Wei, "Research of switch fault diagnosis system based on fuzzy neural network," *Railway Computer Application*, vol. 21, no. 1, pp. 35–39, 2012.

[12] K. Zhang, "The railway turnout fault diagnosis algorithm based on BP neural network," in *Proceedings of the IEEE International Conference on Control Science and Systems Engineering, CCSSE 2014*, pp. 135–138, chn, December 2014.

[13] M. Liu, X. Yan, X. Sun, W. Dong, and Y. Ji, "Fault diagnosis method for railway turnout control circuit based on information fusion," in *Proceedings of the 2016 IEEE Information Technology, Networking, Electronic and Automation Control Conference, ITNEC 2016*, pp. 315–320, May 2016.

[14] S. M. Wang and Y. Lei, "Fault diagnosis for railway switch control circuit based on ARPSO least squares support vector machine," *Journal of Lanzhou Jiaotong University*, vol. 29, no. 4, pp. 1–5, 2010.

[15] V. Atamuradov, F. Camci, S. Baskan, and M. Sevkli, "Failure diagnostics for railway point machines using expert systems," in *Proceedings of the 2009 IEEE International Symposium on Diagnostics for Electric Machines, Power Electronics and Drives, SDEMPED 2009*, fra, September 2009.

[16] H. D. Ardakani, C. Lucas, D. Siegel et al., "PHM for railway system—A case study on the health assessment of the point machines," in *Proceedings of the Prognostics and Health Management (PHM)*, pp. 1–5, June 2012.

[17] Q. He and Y. He, *MATLAB Extended Programming*, Tsinghua University Press, 2002, 340–349.

[18] Y. Li, D. Xue, E. Forrister, G. Lee, B. Garner, and Y. Kim, "Human Activity Classification Based on Dynamic Time Warping of an On-Body Creeping Wave Signal," *IEEE Transactions on Antennas and Propagation*, vol. 64, no. 11, pp. 4901–4905, 2016.

[19] M. Baumann, M. Ozdogan, A. D. Richardson, and V. C. Radeloff, "Phenology from Landsat when data is scarce: Using MODIS and Dynamic Time-Warping to combine multi-year Landsat imagery to derive annual phenology curves," vol. 54, pp. 72–83, 2017.

[20] S. Lu, G. Mirchevska, S. S. Phatak et al., "Dynamic time warping assessment of high-resolution melt curves provides a robust metric for fungal identification," *PLoS ONE*, vol. 12, no. 3, Article ID e0173320, pp. 1–21, 2017.

[21] J. J. Qiu, "Analysis of Action Current Curve of ZD6 Switch Machine," *Railway Signalling Communication*, vol. 4, no. 7, p. pp, 2008.

[22] Q. Guan, "High-speed Railway Switch Failure Diagnosis Based on FOA-LSSVM," *Bulletin of Science and Technology*, vol. 4, pp. 230–232, 2015.

[23] H. Yilboga, Ö. F. Eker, A. Güçlü, and F. Camci, "Failure prediction on railway turnouts using time delay neural networks," in *Proceedings of the 8th IEEE International Conference on Computational Intelligence for Measurement Systems and Applications, CIMSA 2010*, pp. 134–137, ita, September 2010.

[24] Y. M. He, *Research on Fault Diagnosis Method of High-speed Railway Turnouts*, Beijing Jiaotong University, 2014, 1–76.

[25] O. F. Eker, F. Camci, and U. Kumar, "SVM based diagnostics on railway turnouts," *International Journal of Performability Engineering*, vol. 8, no. 3, pp. 289–298, 2012.

[26] O. F. Eker, F. Camci, A. Guclu, H. Yilboga, M. Sevkli, and S. Baskan, "A simple state-based prognostic model for railway turnout systems," *IEEE Transactions on Industrial Electronics*, vol. 58, no. 5, pp. 1718–1726, 2011.

[27] C. Letot, P. Dersin, M. Pugnaioni et al., "A data driven degradation-based model for the maintenance of turnouts: A case study," *IFAC-PapersOnLine*, vol. 28, no. 21, pp. 958–963, 2015.

[28] K. K. Fu, B. L. Zheng, and X. Li, "Method of data extracting of image curve based on matlab," *Journal of Shantou University (Natural Science Edition)*, vol. 27, no. 2, pp. 52–54, 2010.